SPCI 10

10th International Symposium on the Science and Processing of Cast Iron

10-13 NOVEMBER 2014 | MAR DEL PLATA | ARGENTINA

Proceedings

Edited by Roberto BOERI, Juan MASSONE and Graciela RIVERA



>BACKGROUND

The Institute for Research in Materials Science and Technology (INTEMA) hosted the tenth International Symposium on the Science and Processing of Cast Iron (SPCI 10), from 10 to 13th of November 2014.This symposium continued a series which began in Detroit, USA (1964), and was followed by meetings held at Geneva, Switzerland (1974), Stockholm, Sweden (1984), Tokyo, Japan (1989), Nancy, France (1994), Birmingham, USA (1998), Barcelona, Spain (2002), Beijing, China (2006), and Luxor, Egypt (2010).SPCI 10 gathered the world leading researchers in the field of Cast Iron. It was an excellent forum where scientists, metallurgists, producers as well as users could discuss the state of the art of cast iron science and processing and exchange ideas and experiences. Nowadays Cast Iron, as most engineering materials on earth, faces a strong competition from other materials. Thanks to the joint efforts of producers, technologists and researchers, Cast Iron has not just maintained a strong position in the cast metals market over the last troubled years, but has also gained new markets and increased its applications. SPCI 10 provided an excellent opportunity to learn about the latest developments and to foresee the near future in this field.

ORGANIZATION

Chairman: Dr. Roberto Boeri *(UNMdP)*
Co-Chairman: Dr Juan M. Massone *(UNMdP)*

SCIENTIFIC COMMITTEE

- M. Nili Ahmadabadi *(University of Tehran, Iran)*
- Sarum Boonmee *(Suranaree University of Technology, Thailand)*
- Andriy Burbelko *(AGH Univ of Science and Technology, Poland)*
- Manuel Castro *(CINVESTAV, Mexico)*
- Jeong-Kil Choi *(KITECH, Korea)*
- Attila Diószegi *(Jönköping University, Sweden)*
- Hasse Fredriksson *(KTH, Sweden)*
- Marcin Gorny *(AGH Univ of Science and Technology, Poland)*
- Wojciech Kapturkiewicz *(AGH Univ. of Sci. and Technology, Poland)*
- Jacques Lacaze *(CIRIMAT, ENSIACET, France)*
- Frans Mampaey *(Sirris, Belgium)*
- Primož Mrvar *(University of Ljubljana, Slovenia)*
- Vladimir Naydek *(PTIMA, Ukraine)*
- Adel Nofal *(CMRDI, Egypt)*
- Von Richards *(Missoury Univ of Science and Technology, USA)*
- Iulian Riposan *(Univ Polytechnica of Bucharest, Romania)*
- András Roósz *(University of Miskolc, Hungary)*
- Peter Schumacher *(Austrian Foundry Research Institute, Austria)*
- Oleg I. Shinsky *(PTIMA, Ukraine)*
- Carlos Silva Ribeiro *(University of Porto, Portugal)*
- Torbjørn Skaland *(Elkem, Norway)*
- Doru M. Stefanescu *(Ohio State Univ; Univ. of Alabama, USA)*
- Ramón Suárez *(Azterlan, Spain)*
- Guoxiong Sun *(Southeast University, China)*
- Ingvar Svensson *(Jönköping University, Sweden)*
- Edis Ten *(MISIS, Moscow, Russia)*
- Niels Skat Tiedje *(Technical University of Denmark, Denmark)*
- Babette Tonn *(TU Clausthal, Germany)*
- Adian Udroiu *(Italy)*
- R. C. Voigt *(Pennsylvania State University, USA)*
- Jiandong XING *(Xi´an Jiaotong University, China)*
- Zenon Ignaszak, *(Poznan University of Technology, Poland)*
- Roberto Boeri *(UNMdP-CONICET, Argentina, Chairman)*
- Juan M. Massone *(UNMdP-CONICET, Argentina, Co-chairman)*

ORGANIZING COMMITTEE

- Prof. Graciela Rivera *(UNMdP-CONICET)*
- Prof. Ricardo Martínez *(UNMdP-CONICET)*
- Prof. Martín Caldera *(UNMdP-CONICET)*
- Prof. Alejandro Basso *(UNMdP-CONICET)*
- Prof Ricardo Dommarco *(UNMdP-CONICET)*
- Dr. Sebastián Laino *(UNMdP-CONICET)*

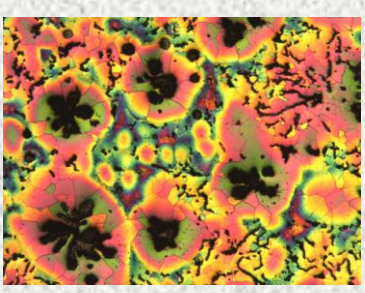

TOPICS

SPCI 10 discussed the current status of:

- Fundamental research on solidification and solid state transformations of cast iron
- Recent technologies of melting, casting, heat treatment and process control.
- Computational modeling of cast iron transformations and processing.
- Novel developments and applications of cast iron.
- Mechanical properties of Cast Iron.

PUBLICATIONS

Boron Effect on the Precipitation of Secondary Carbides During Destabilization of a High-Chromium White Iron

A. Bedolla-Jacuinde[1], F. V. Guerra[1], I. Mejía[1], J. Zuno-Silva[2], C. Maldonado[2]
[1]Universidad Michoacana de San Nicolás de Hidalgo, México
[2]Universidad Autónoma del Estado de Hidalgo, México

This work analyses the secondary carbides precipitation during the destabilization of a 17%Cr white iron containing 195 ppm Boron. The experimental iron was characterized in the as-cast conditions to have comparable parameters with the heat treated samples. Destabilization heat treatments were undertaken at temperatures of 825, 900 and 975ºC for 25 minutes; each sample was air cooled after this soaking time. Characterization was undertaken by optical and electronic microscopy, image analysis and EDS microanalysis; hardness and microhardness were also evaluated. It was found that the volume fraction of secondary carbides precipitated is always higher for the lowest destabilization temperature (825ºC) due to the lower carbon solubility in austenite at low temperatures. A much higher precipitation for the irons containing boron than that for the iron without boron at any destabilization temperature was also noticed.
For the iron containing boron, a density of 23 carbide particles per square micron was measured when destabilized at 825ºC, and it decreased to about 10 particles per square micron when destabilized at 975ºC. In the case of the alloy without boron additions, about 10 carbides per squared micron were counted when destabilized at 825ºC and about 5 when destabilized at 975ºC. Higher volumes of carbide precipitation implies higher values of bulk hardness and microhardness in the alloys. The results suggest that boron works as nuclei for the precipitation of secondary carbides; this is discussed in terms of the limited solubility of boron in iron and the formation of boron rich precipitates found in the iron in the as-cast conditions.

Introduction

High-chromium white irons are ferrous alloys containing between 11-30%Cr and 1.8-3.6%C. It is also common to find some alloying elements such as molybdenum, manganese, copper, and nickel. The typical as-cast microstructure of these alloys consists of primary and/or eutectic carbides (M_7C_3) in a metastable austenitic matrix[1]. The hard eutectic carbides are mainly responsible for the good abrasion resistance of these alloys. Therefore, these alloys have been widely used for applications where stability in severe environments is the main requirement, such as the mineral processing industry, cement and paper production, and the steel manufacturing industry[2]. Both carbides and matrix contribute to wear resistance and fracture toughness. Eutectic carbides have a hexagonal close-packed (hcp) crystalline structure and solidify as colonies of plates or bars (eutectic grains). Once solidified, carbide morphology is relatively immune to a subsequent modification by heat treatment. The as-cast austenitic structure, in contrast, is readily heat treated for destabilization and for obtaining small secondary carbides precipitated in a matrix that is a mixture of martensite and retained austenite[3].

The commonly applied heat treatment for maximum strengthening is denoted as "destabilization", which consists of heating the alloy at temperatures within 800-1100°C, soaking at these temperatures, followed by an air quenching at room temperature. During soaking, carbon and chromium from the matrix react to form small carbide particles. The new chromium- and particularly, carbon-depleted matrix readily transforms to martensite during the subsequent cooling down. Therefore, the final structure after destabilization consists of M_7C_3 eutectic carbides and a martensitic matrix with secondary carbides distributed in it[1]. Secondary carbide precipitation and the transformed martensitic matrix promote an even more brittle alloy. However, a martensitic matrix is recommended to obtain greater hardness and better wear properties; but this increase in hardness affects fracture toughness. Such a phenomenon brings attention to the importance of operation factors of the destabilization treatment to be studied to determine the appropriate temperature and soaking time for such a high level of hardness and fracture toughness.

Corresponding autor: abedollj@umich.mx

Although relatively little systematic research on the secondary carbide precipitation phenomena and their effect on the iron matrix has been developed, some works regarding this field are relevant[4-9].

Experimental Procedure

The experimental white iron for the present work was made in an induction furnace by using high purity raw materials, therefore obtaining an impurities free well-controlled chemical composition alloy. Boron was added to the melt at the latest stage of the melting process. The melt was poured at 1450 °C into sand moulds and squared cross section bars of 25 x 25mm were obtained. The bars were sectioned with an alumina abrasive cutting wheel in a DISCOTOM by copious water amounts. The cutting process, manually controlled, was as slow as possible to avoid overheating the sample and rectangular 12 × 12 × 4 mm samples were obtained.

Destabilization heat treatments were undertaken in an electric furnace in an air atmosphere. The samples were placed into the furnace for heat treatment; once the desired temperature was reached, the samples were soaked for 25 min and then taken out and water quenched to ensure that the secondary carbides had precipitated during the soaking time only. Heat treatments were undertaken at 825, 900, and 975°C.

Materials characterization in both as-cast and heat treated conditions was undertaken by optical and electronic microscopy, energy dispersive spectroscopy (EDS) microanalysis, X- ray diffraction (XRD), and image analysis. Samples were prepared for metallography in the traditional way: grinding on abrasive paper of different mesh sizes (80, 180, 320, 400, 600, and 1200). Samples were then polished on nylon cloth with 6 µm diamond paste as the abrasive and then with 1 µm paste. Etching was carried out with two different solutions depending on the purpose: Villela's etchant (5 ml HCl and 1 g picric acid in 100 ml ethanol) for 30-60 s to reveal the microstructure, and a solution of 50 ml $FeCl_3$ plus 20 ml HCl in 930 ml ethanol, where the samples were immersed for about 3 h, for deep etching. This latter etching readily removes part of the matrix on the surface, allowing the naked carbides to be observed.

As-cast eutectic carbide volume fraction was measured by image analysis on digitized micrographs obtained at 250X on a Nikon EPHIPHOT 3000 inverted metallurgical microscope. For this purpose, the samples were deeply etched, and 20 micrographs were processed by image analysis. XRD studies were also undertaken to identify the different phases present in the alloy both before and after heat treatment. Retained austenite quantification was also calculated by XRD data by the technique described by Kim[10]. XRD tests were carried out by using Cu-Kα radiation in a 2θ range of 30-100°. Further characterization was undertaken on a JEOL 6400 SEM at 20 kV for imaging and microanalysis, and a PHILIPS TECNAI TEM. Secondary carbides volume fraction and size was obtained by point counting measurements on SEM micrographs by using a transparent 250 point grid.

Bulk hardness and microhardness of the matrix were undertaken on metallographic samples. Twenty tests for each sample were carried out by a diamond indenter and a 50 g load for 15 s, for Vickers microhardness (HV50). Bulk hardness was undertaken in the Rockwell C scale.

Results and Discussion

The microstructure of the experimental alloy has been widely described in a previously published paper[11]. It was observed that when boron increases in the iron, the volume fraction of matrix decreased. This suggests that boron additions displace the composition closer to the eutectic. DTA analysis from the same work supports this assumption, since the starting solidification temperature was observed to decrease and the solidification range was narrower for the irons with boron additions. An additional microstructural refinement was also observed when boron was increased due to the shorter solidification range.

Boron also increased the carbide volume fraction, refined the microstructure and increased the diameter of the eutectic carbide bars. These phenomena were explained in terms of the boron segregation and its partition to the carbide phase. Fig. 1 shows the as-cast microstructure of the irons containing no boron (a), 93 ppm boron (b) and 195 ppm boron (c). For the present study, only the irons with no boron and that with 195 ppm boron were used.

Corresponding autor: abedollj@umich.mx

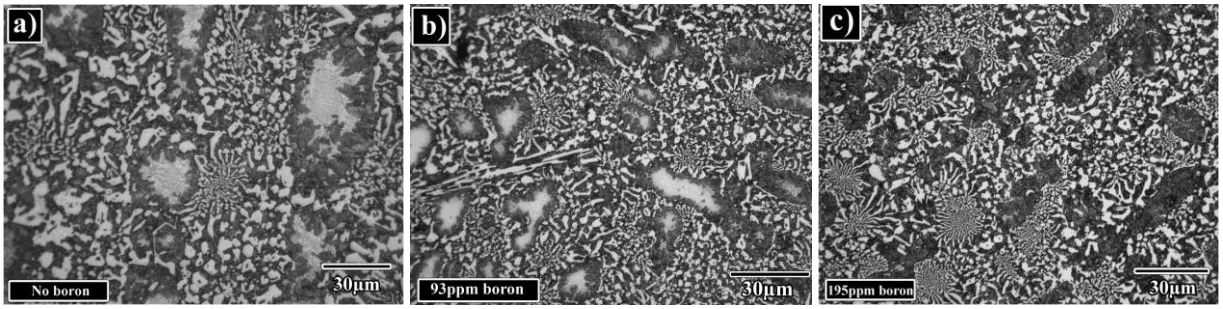

Fig. 1: As-cast microstructure of the irons showing the effect of boron as a microstructural refinement(11).

As mentioned before, the structure of the material for this study consists of a network of eutectic carbides of the type M_7C_3 embedded into a metastable austenitic matrix. Due to the addition of elements (C, Cr, Ni and Mo) that increase hardenability, it is possible to get austenite at room temperature. Such austenite is saturated in chromium, carbon and boron (just in the case of the alloy with boron additions).

Heat treatments were undertaken at temperatures of 825, 900 and 975° C and a soaking time of 25 min for the iron with no boron and for the iron with 195 ppm boron. The destabilization treatment promoted the secondary carbide precipitation within the matrix in each iron; Figure 2 shows a sequence of SEM micrographs where the effect of destabilization temperature is evident on the level of secondary carbides precipitation.

From the sequence of micrographs in Fig. 2, a higher secondary carbide precipitation is evident in the irons treated at 825°C and the amount of such carbides decreased as the temperature increased. Such an effect can be explained by observing the Fe-C diagram, and particularly the line of solubility of carbon in austenite. At low temperatures, in the range where austenite is stable, the amount of carbon in equilibrium in austenite is lower than for higher temperatures. Before the heat treatment, austenite is saturated with carbon and chromium; therefore, the amount of elements that precipitate (particularly carbon) is higher for lower temperatures. On the contrary, at higher temperatures austenite dissolves higher amounts of carbon and just a reduced amount of this element is available for precipitation.

On the other hand, the amount of secondary carbides also increased for the boron added iron at any destabilization temperature (see micrographs in Fig. 1). This suggests that the secondary carbide formation by carbon and chromium is favoured by the presence of boron, as it occurs for the eutectic carbides during the solidification process[11].

In order to measure the level of secondary carbides precipitation, higher magnification SEM micrographs were obtained (see Fig. 3). From these pictures, the amount and size of secondary carbides were measured to give numerical values to the precipitation phenomenon and to complement the observations on the micrographs.

The reason for which a higher precipitation of secondary carbides in the iron with boron additions may be explained according to the following theories: Powell and Bee[9] and Bee *et al.*[12], found that the secondary carbides precipitate on slip bands or sub-grain boundaries in the austenitic regions. Such slip bands and sub-grain boundaries are formed due to the dislocations that form by the differences in thermal coefficients of carbides and matrix. On the other hand, by using an electronic theory of functional density, Chen *et al.*[13] have analysed the effect of boron as an impurity at the dislocations in bcc iron. Energetic calculus, indicate that boron has a strong tendency to segregate towards the faults formed in the direction of the dislocation lines known as "kinks". The calculation is based on structural energy, atomic energy, partial density of state, and the difference in charge density. Results of energy indicate that boron located in kinks has a high structural stability, while its presence in an iron neighbourhood strongly increases the interatomic energy between boron and the iron atoms located at the kinks. Since the secondary carbides precipitate at slip bands and sub-grain boundaries, the presence of boron at these lines promotes the precipitation of secondary carbides by generating high energy points.

Corresponding autor: abedollj@umich.mx

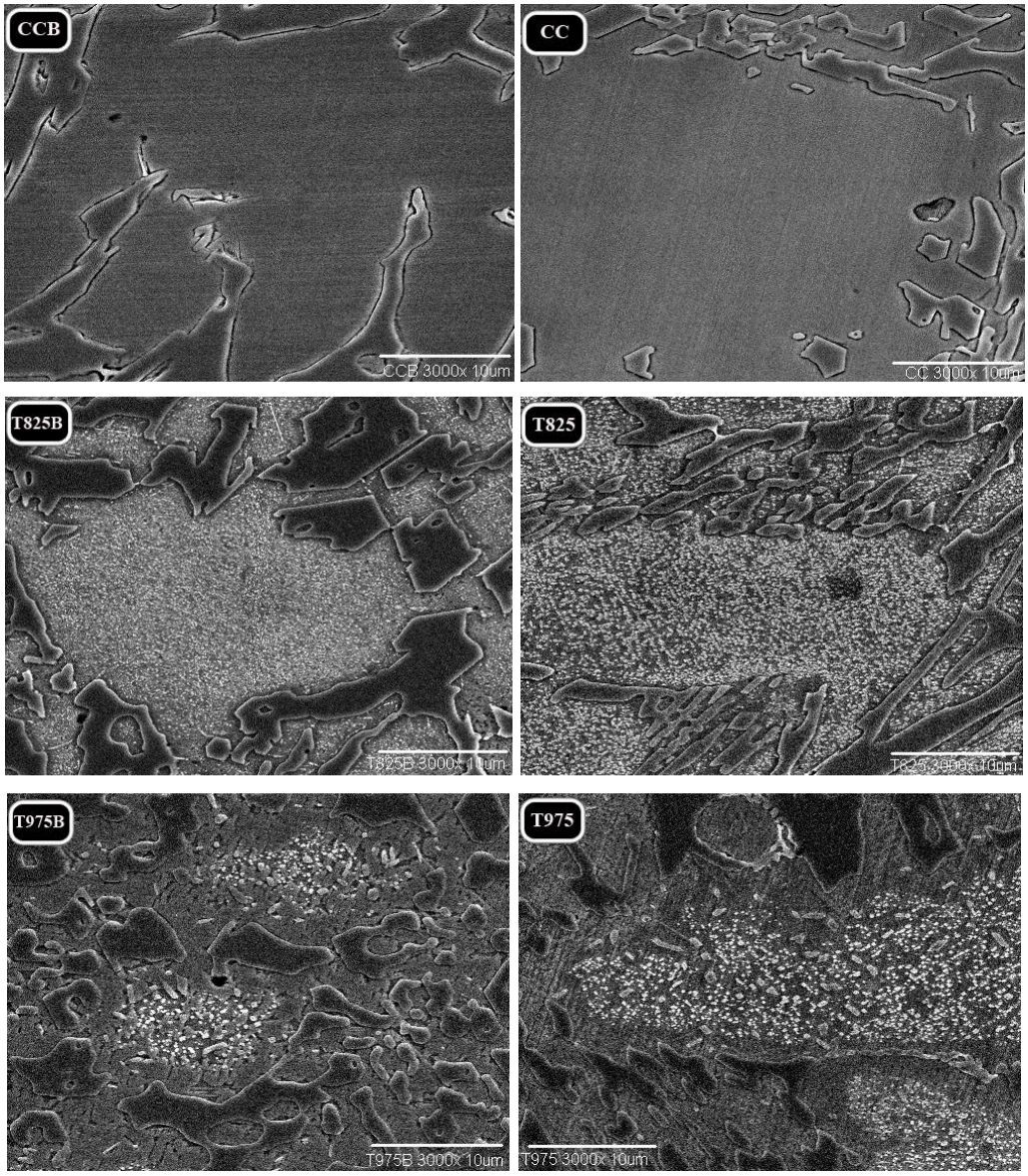

Fig. 2: Sequence of SEM micrographs of the experimental irons after destabilization treatments at different temperatures. (CC= as-cast, T825= destabilization temp 825ºC, T975=destabilization temp 975ºC, B= Boron added).

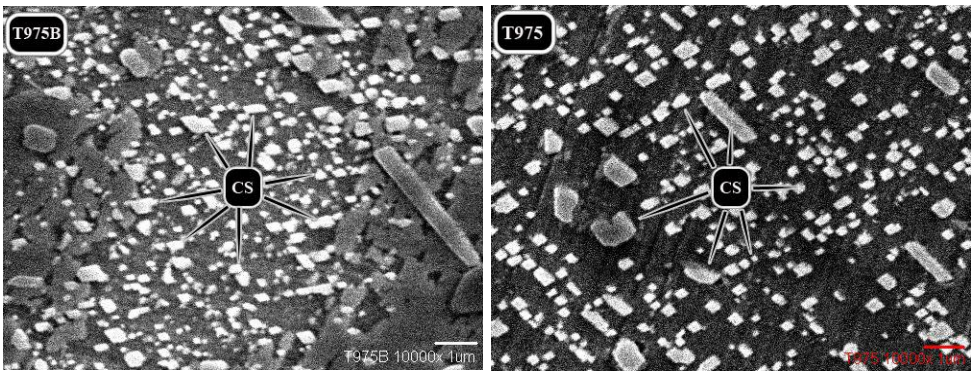

Fig. 3: SEM micrographs used for the measurement of the secondary carbide precipitation.

Corresponding autor: abedollj@umich.mx

Fig. 4 shows the number of secondary carbides precipitated in a square micron as a function of the destabilization temperature. From this graph, the higher amount of carbides for the iron with no boron additions is evident, the iron heat treated at 825°C, shows about 10 carbides in a square micron and when heat treated at 975°C the amount of carbides is just 5. For the case of the iron with 195 ppm boron, the density of carbides is about 22 in a square micro when heat treated at 825°C; and just 8 carbides per square micron when heat treated at 975°C. It can be observed that the level of precipitation is always higher for the boron added iron; it has been suggested that boron increases the activity and diffusion of carbon in iron in the same way silicon does in ductile and grey irons. Under these conditions, a higher mobility of carbon promotes higher precipitation, such effect seems to be stronger at lower temperatures, since at higher temperatures, diffusion is higher and the effect of the temperature on this phenomenon is stronger than the composition. Additionally, the size of the precipitated carbides is affected with the treatment temperature. From the microstructures of Fig. 2 and the graph in Fig. 5 it can be seen that the secondary carbides are finer for lower temperatures and increase in size as temperature increases. Again, this phenomenon is associated with a higher diffusion at higher temperatures and to an Oswald ripening process[14]. Note that the carbides are always finer for the boron added iron.

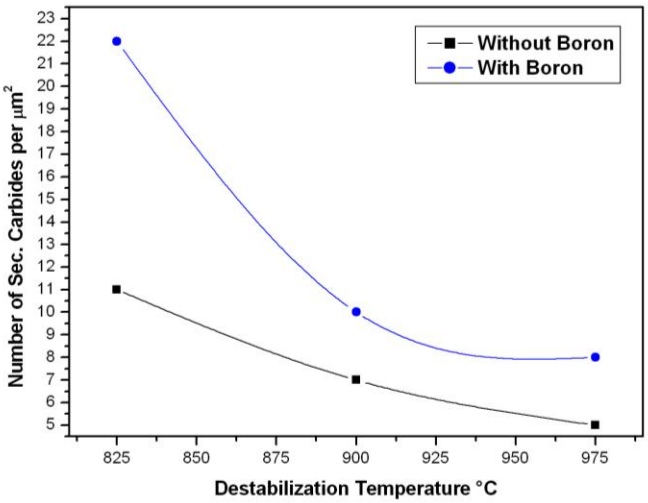

Fig. 4: Number of secondary carbides precipitated in a square micron after destabilization at different temperatures.

It is expected, that when the precipitation process occurs in the matrix of the irons, the tribological properties increase. This is attributed to the strengthening of matrix due to the presence of these secondary carbides and also the amount of martensite formed from austenite during cooling after the destabilization treatment. Such microstructural changes are associated with an increase in the hardness of the alloys.

Fig. 6 shows the hardness values as a function of the destabilization treatment. In the as-cast conditions, hardness was 38 and 40 HRC for the irons with no boron ant for the one with 195 ppm boron respectively. When heat treated at 875ºC, hardness was 56 HRC for the boron added iron and 53 HRC for the iron without boron. When heat treated at 975ºC, hardness decreased to 43 and 42 HRC respectively. Similarly, a decrease in microhardness of the matrix was observed for both irons when increased the treatment temperature (see Fig. 7). When heat treated at 825ºC, microhardness was $800HV_{15}$ for the iron with boron additions and $550HV_{15}$ for the no boron added iron. When heat treated at 975ºC, microhardness decreased to $425HV_{15}$ for the boron added iron and to 375 for the no boron added iron. Such decrease in hardness and microhardnessis related to the minor amount of secondary carbides and to the increase in retained austenite as described later, since the volume fraction of eutectic carbides is constant for each iron, and only the matrix transforms.

XRD analysis (Fig. 8) indicates that the secondary carbides that precipitate are of the type M_7C_3, the same type of the eutectic carbides. The type of the carbides that precipitate depends on the composition of the alloy and on the destabilization temperature[15,16]. Alloys with chromium contents higher than 25% precipitate carbides of the type $M_{23}C_6$ [2,17] as fine interconnected bars. On the other hand, with chromium levels of 15-20% the carbides are of the type M_7C_3 as bars and plates[17]. These observations are in agreement with the present study.

Corresponding autor: abedollj@umich.mx

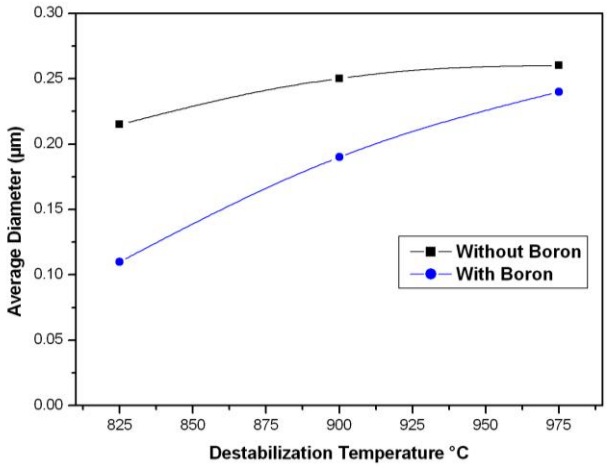

Fig. 5: Average size of the secondary carbides precipitated after destabilization treatment.

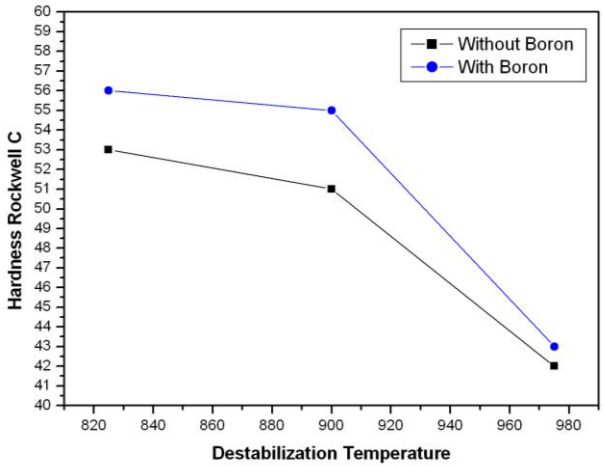

Figure 6.- Hardness Rockwell C as a function of the destabilization temperature.

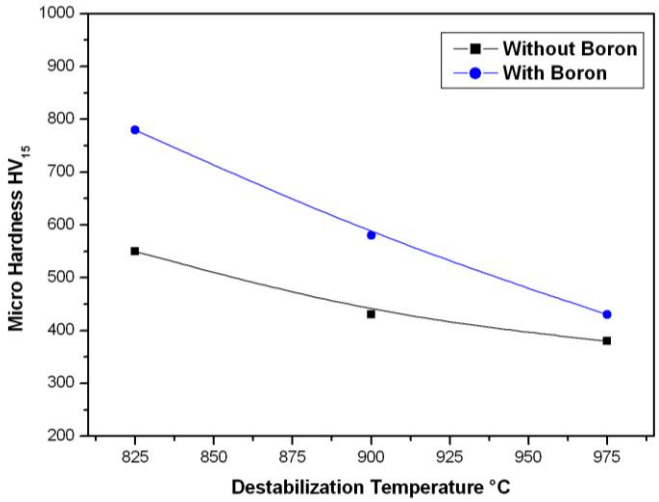

Fig. 7: Vickers$_{15}$ Microhardness of matrix as a function of the destabilization temperature.

Corresponding autor: abedollj@umich.mx

It has been reported that secondary carbides commonly precipitate in slip bands or sub-grain boundaries within the eutectic regions[18,19]. Such slip bands and sub-grain boundaries are formed due to residual stresses generated by the different thermal expansion coefficients of eutectic carbides and the austenitic matrix. Kuwano *et al*.[20] also noted that in irons with a low Cr/C ratio, the secondary carbides precipitated within the dendrites; while for high Cr/C ratios the secondary carbides precipitated preferentially adjacent to the eutectic carbides. In the present work, the secondary carbides precipitate uniformly in the whole matrix at any treatment temperature.

Hardenability in the destabilized structure is generally lower than that for the as-cast alloy due to the reduction of alloying elements by the precipitation process of secondary carbides. The chromium content is used to generate a determined eutectic carbide volume in the iron[21] and the residual chromium dissolved in matrix contributes to hardenability. After heat treatment, the reduced amount of chromium and carbon dissolved in the matrix promotes the austenite transformation. However, the presence of nickel and molybdenum partially compensates such a decrease in hardenability. Therefore, the final structure of matrix is composed of martensite, retained austenite and of course the precipitated secondary carbides.

The precipitation of secondary carbides diminishes the amounts of chromium and carbon dissolved in the matrix. Such a low alloying content, increases the M_S temperature so during the subsequent cooling down, most of the austenitic matrix transforms to martensite (see the XRD from Fig. 8). However, some retained austenite remains in the structure, which depends on the carbon content after destabilization, which in turn is influenced by the alloying elements present and the time and temperature of destabilization heat treatment[2,21,22].

The amount of residual austenite after heat treatment, as calculated by XRD studies by using the method described by Kim[10], is shown from Fig. 9 shows.

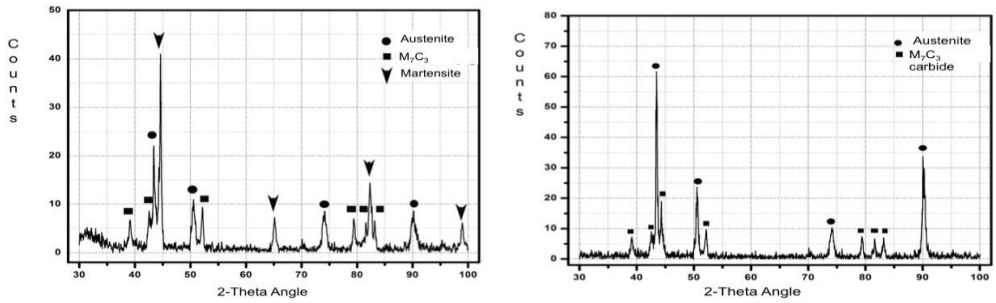

Fig 8: XRD traces for the iron with boron additions, a) as-cast and b) heat treated at 900ºC. Note the presence of martensite and the diminution of austenite after heat treatment.

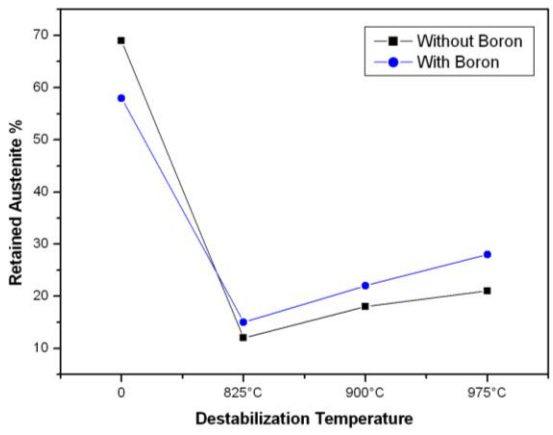

Fig. 9: Retained austenite as a function of the destabilization temperature for the two experimental irons.

In the as-cast irons, the amount of austenite is about 70% for the iron without boron and about 60% for the boron added iron. After the destabilization treatment at 825ºC, retained austenite is between 10 and 15% and increased to 20-25% when destabilized at 975ºC. According to the results shown in Fig. 9, at the destabilization

Corresponding autor: abedollj@umich.mx

temperature of 825ºC, where the higher precipitation of secondary carbides was obtained, less retained austenite was observed. On the contrary, at higher destabilization temperatures, where the precipitation is lower, higher amounts of retained austenite were observed. Lower precipitation means higher amounts of dissolved carbon in austenite; this higher amount of dissolved carbon raises the M_S temperature and a major amount of retained austenite is obtained. It means less amount of austenite is transformed to martensite. For the iron with no boron additions a major austenite to martensite transformation is produced compared with the boron-added iron. This is due to the behaviour of boron that can substitute carbon in the carbide phase; therefore, a higher amount of carbon remains dissolved before cooling down. The presence of retained austenite and martensite is observed from TEM micrographs in Figure 10 where bright field, dark field and an electron diffraction pattern from the plane of martensite are shown.

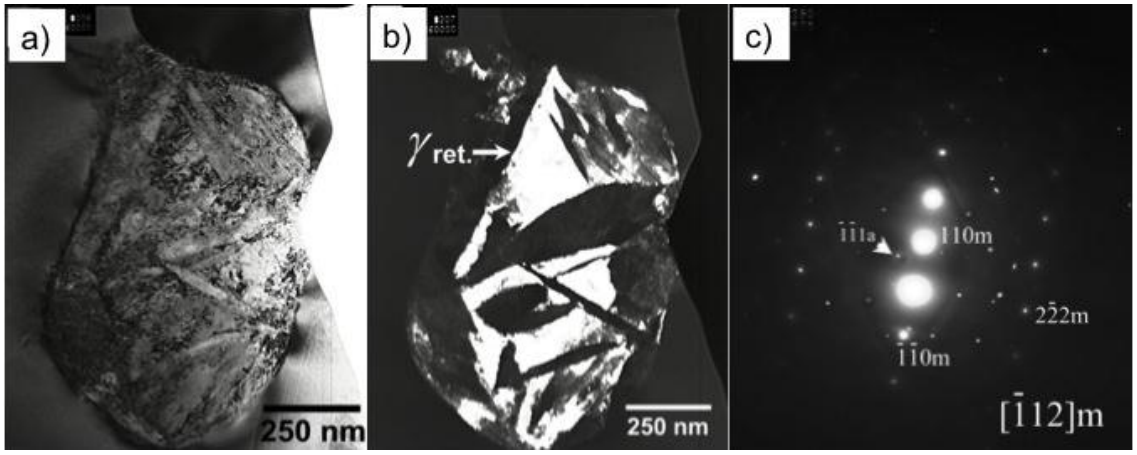

Fig. 10: Bright field and dark field TEM images showing the presence of retained austenite in the heat treated boron added iron. a) Bright field of matrix, b) Dark field of the same matrix generated by (-1-11) spot of austenite arrowed in the selected area diffraction (SAD) pattern from [-112] of martensite shown in c).

Conclusions

1. During the undertaken heat treatments for the precipitation of secondary carbides, the iron with 195 ppm boron shows better response to the destabilization treatment since the amount of secondary carbides is higher and finer in size than the iron with no boron additions at any destabilization temperature. In addition, it was found that the temperature at which there are higher amounts of secondary carbides is 825°C; nonetheless, diffusion is slower than that at higher temperatures (900 and 975°C), the amount of carbon available for the carbides precipitation is higher at low temperatures since the equilibrium solubility of carbon in austenite decreases with the temperature.
2. According to the measurements of retained austenite, a higher amount of austenite is obtained in the boron added iron since during the precipitation of the secondary carbides; carbon may be substituted by boron in these secondary carbides. Therefore, less carbon is used to form the secondary carbides and a higher amount of carbon remains dissolved in matrix, which in turn promotes an increase in the M_S temperature. This increase diminishes the amount of austenite to be transformed to martensite.
3. It was observed that for the alloy with boron additions, this element acts as promoter of the secondary carbides. It is suggested that boron, according to its nature, is located preferentially at the "kinks" in the dislocation lines. Although, secondary carbides also precipitate at slip bands or sub-grain boundaries generated by dislocations. According to these observations, it can be assumed that the presence of boron at the dislocation lines enhances the precipitation of secondary carbides due to the high energy associated between the boron atoms and their iron neighbours.

Corresponding autor: abedollj@umich.mx

References

1. C.P Tabrett, I.R. Sare, and M.R. Gomashchi, *International Materials Reviews*, 1996, vol. **41**, No. 2, pp. 59-82.
2. O.N. Dogan, J.A. Hawk and G. Laird II, *Metallurgical and Materials Transactions A*, 1997, vol. **28**, pp. 1315-1327.
3. G. Laird and G. Powell, *Metallurgical Transactions A*, 1993, **24**(2) pp. 981-988.
4. W.W.Cias, *AFS Transactions*,1974, **82** pp. 317-328.
5. G. Powell and G. Laird, *Journal of Materials* Science, 1992, **27**, pp. 29-35.
6. F. Maratray and A. Poulalion, *AFS Transactions*, 1982, **90**, pp. 795-804.
7. J.T.H. Pearce, AFS Transactions, 1984, **92**, pp. 599-621.
8. M. Kuwano, K. Ogi, A. Sawamoto, *AFS Transactions*, 1990, **98**, pp. 725-734.
9. G.L.F. Powell and J.V. Bee, *Journal of Materials Science*, 1996, **31**, pp. 707-711.
10. C. Kim: *J. Heat Treating*, 1979, **1**(2), pp. 43-51.
11. R. Correa, A. Bedolla-Jacuinde, I. Mejía, E. Cardoso and B. Hernández, *International Journal of Cast Metals Research*, **24**(2011) pp. 37-44.
12. J.V.Bee, G.L.F. Powell and B. Bednarz, *Scripta Metallurgica et Materialia*, 1994, vol. **31**, pp. 1735-1736.
13. L.Q. Chen, Z.C. Qiu, C.Y. Wang and T. Yu, *J. of Alloys and Compounds*, **428**, (2007) pp. 49-53.
14. P.W. Voorhees, *Journal of Statistical Physics*, vol. **38**, (1985) p. 231-252.
15. ASTM A532-93 Philadelphia, P A, ASTM, 1999, vol. **1.02**, pp. 282-285.
16. A. Bedolla-Jacuinde, R. Correa, J.G. Quezada, C. Maldonado, *Materials Science and Engineering* A398 (2005) pp. 297-308.
17. A. Sawamoto, K. Ogi and K. Matsuda, *AFS Transactions*, 1986, vol. **94**, pp. 403-416.
18. G. Laird, R. Gundlach and K. Röhring American Foundry Society, Des Plaines Illinois 60016-8399.
19. S. Jackson, *Journal of the Iron and Steel Institute*, 1970, vol. **204**, pp. 163-167.
20. M. Kuwano, K. Ogi, A. Sawamoto, and K. Matsuda*AFS Transactions*, 1990, vol. **98**, pp. 725-734.
21. F. Maratray, *AFS Transactions*, 1971, vol.**79**, pp. 121-124.
22. M. Radulovic, M. Fiset, K. Peev, and M. Tomovic, , *Journal of Materials Science*, 1994, vol. **29**, pp. 5085-5094.

Acknowledgements

The authors gratefully acknowledge the National Council for Science and Technology of Mexico (CONACYT) and the Universidad Michoacana (UMNSH) for the financial support for the development of the present work.

Corresponding autor: abedollj@umich.mx